An adjustable, safe and highly protective live-attenuated SARS-CoV-2 vaccine based on large-scale one-to-stop codon modifications

Martin Beer (Martin.Beer@fli.de)
Friedrich-Loeffler-Institute https://orcid.org/0000-0002-0598-5254

Jacob Schön
Institute of Diagnostic Virology, Friedrich-Loeffler-Institut, Federal Research Institute of animal health
https://orcid.org/0000-0002-9801-7972

Güliz Barut
Institute of Virology and Immunology (IVI), Bern and Mittelhäusern; Department of Infectious Diseases and Pathobiology, Vetsuisse Faculty, University of Bern

Bettina Trüeb
Institute of Virology and Immunology (IVI), Bern and Mittelhäusern; Department of Infectious Diseases and Pathobiology, Vetsuisse Faculty, University of Bern

Nico Halwe
Friedrich Loeffler Institut https://orcid.org/0000-0002-7983-2808

Inês Veiga
Institute of Virology and Immunology (IVI), Bern and Mittelhäusern; Department of Infectious Diseases and Pathobiology, Vetsuisse Faculty, University of Bern

Annika Kratzel
Institute of Virology and Immunology (IVI), Bern and Mittelhäusern; Department of Infectious Diseases and Pathobiology, Vetsuisse Faculty, University of Bern

Lorenz Ulrich
Institute of Diagnostic Virology, Friedrich-Loeffler-Institut, Federal Research Institute of animal health
https://orcid.org/0000-0001-5004-806X

Jenna Kelly
University of Bern

Melanie Brügger
Institute of Virology and Immunology (IVI), Bern and Mittelhäusern; Department of Infectious Diseases and Pathobiology, Vetsuisse Faculty, University of Bern

Claudia Wylezich
Institute of Diagnostic Virology, Friedrich-Loeffler-Institut, Federal Research Institute of animal health
https://orcid.org/0000-0002-0436-4480

Adriano Taddeo

Institute of Virology and Immunology https://orcid.org/0000-0003-3281-1548

Etori Moreira

Institute of Virology and Immunology (IVI), Bern and Mittelhäusern; Department of Infectious Diseases and Pathobiology, Vetsuisse Faculty, University of Bern

Péter Túrós

Department of Infectious Diseases and Pathobiology, Bern; Graduate School for Biomedical Science, University of Bern; Institute of Animal Pathology, University of Bern

Llorenç Grau-Roma

Institute of Animal Pathology, University of Bern https://orcid.org/0000-0002-9406-8844

Ann Kathrin Ahrens

Institute of Diagnostic Virology, Friedrich-Loeffler-Institut, Federal Research Institute of animal health

Kore Schlottau

Institute of Diagnostic Virology, Friedrich-Loeffler-Institut, Federal Research Institute of animal health https://orcid.org/0000-0002-3999-0393

Tobias Britzke

Department of Experimental Animal Facilities and Biorisk Management, Friedrich-Loeffler-Institut, Federal Research Institute of animal health

Angele Breithaupt

Friedrich-Loeffler-Institut https://orcid.org/0000-0002-6373-5923

Blandina Exteves

Institute of Virology and Immunology (IVI), Bern and Mittelhäusern; Department of Infectious Diseases and Pathobiology, Vetsuisse Faculty, University of Bern

Lea Almeida

Institute of Virology and Immunology (IVI), Bern and Mittelhäusern; Department of Infectious Diseases and Pathobiology, Vetsuisse Faculty, University of Bern https://orcid.org/0009-0007-9945-0894

Lisa Thomann

Institute of Virology and Immunology (IVI), Bern and Mittelhäusern; Department of Infectious Diseases and Pathobiology, Vetsuisse Faculty, University of Bern https://orcid.org/0000-0003-3530-0524

Christelle Devisme

Institute of Virology and Immunology (IVI), Bern and Mittelhäusern; Department of Infectious Diseases and Pathobiology, Vetsuisse Faculty, University of Bern

Hanspeter Stadler

Institute of Virology and Immunology (IVI), Bern and Mittelhäusern; Department of Infectious Diseases and Pathobiology, Vetsuisse Faculty, University of Bern

Silvio Steiner

Institute of Virology and Immunology (IVI), Bern, Switzerland; Department of Infectious Diseases and Pathobiology, Vetsuisse Faculty, University of Bern, Bern, Switzerland; Graduate School for Cellu https://orcid.org/0000-0003-1999-1425

Sarah Ochsenbein

Institute of Virology and Immunology (IVI), Bern and Mittelhäusern; Department of Infectious Diseases and Pathobiology, Vetsuisse Faculty, University of Bern

Kimberly Schmied

Institute of Virology and Immunology (IVI), Bern and Mittelhäusern; Department of Infectious Diseases and Pathobiology, Vetsuisse Faculty, University of Bern https://orcid.org/0000-0002-6158-7074

Fabien Labroussaa

Institute of Veterinary Bacteriology, Vetsuisse Faculty, University of Bern; Department of Infectious Diseases and Pathobiology, Vetsuisse Faculty, University of Bern

Jörg Jores

University of Bern https://orcid.org/0000-0003-3790-5746

Philip V´kovski

RocketVax AG, Basel

Vladimir Cmiljanovic

RocketVax AG, Basel

Maro Alves

Institute of Virology and Immunology (IVI) Bern and Mittelhäusern; Department of Infectious Diseases and Pathobiology; Multidisciplinary Center for Infectious Diseases, University of Bern

Charaf Benarafa

Institute of Virology and Immunology (IVI) Bern and Mittelhäusern; Department of Infectious Diseases and Pathobiology; Multidisciplinary Center for Infectious Diseases, University of Bern

Donata Hoffmann

Friedrich Loeffler Institute https://orcid.org/0000-0003-4552-031X

Nadine Ebert

Institute of Virology and Immunology (IVI), Bern and Mittelhäusern; Department of Infectious Diseases and Pathobiology, Vetsuisse Faculty, University of Bern

Volker Thiel

Article

Keywords:

Posted Date: August 29th, 2023

DOI: https://doi.org/10.21203/rs.3.rs-3171636/v1

Additional Declarations: Yes there is potential Competing Interest. Related to this work, the University of Bern has filed a patent application for the use of OTS-206 and OTS-228 as vaccine. In this application, J.S., G.T.B., B.S.T., N.J.H., A.K., L.U., F.L., J.J., N.E., D.H., M.B., and V.T. are named as inventors. The

University of Bern and the Friedrich-Loeffler Institute are collaborating with RocketVax AG for the development of OTS vaccines and receive funding for research. V.T. is consulting for RocketVax AG. P.V. and V.C. are employees of RocketVax AG

Title: An adjustable, safe and highly protective live-attenuated SARS-CoV-2 vaccine based on large-scale one-to-stop codon modifications

Short title: SARS-CoV-2 attenuation by one-to-stop codon modification

Authors:

Jacob Schön†[1], G. Tuba Barut†[2,3], Bettina Salome Trüeb†[2,3], Nico Joel Halwe[1], Inês Berenguer Veiga[2,3], Annika Kratzel[2,3], Lorenz Ulrich[1], Jenna N. Kelly[2,3,4,5], Melanie Brügger[2,3], Claudia Wylezich[1,6], Adriano Taddeo[2,3], Etori Aguiar Moreira[2,3], Péter Demeter Túrós[3,7,8], Llorenç Grau-Roma[8], Ann Kathrin Ahrens[1], Kore Schlottau[1], Tobias Britzke[6], Angele Breithaupt[6], Blandina I. Oliveira Esteves[2,3], Lea Almeida[2,3], Lisa Thomann[2,3], Christelle Devisme[2,3], Hanspeter Stalder[2,3], Silvio Steiner[2,3], Sarah Ochsenbein[2,3], Kimberly Schmied[2,3], Fabien Labroussaa[4,9], Jörg Jores[4,9], Philip V'kovski[10], Vladimir Cmiljanovic[10], Marco P. Alves[2,3,4], Charaf Benarafa[2,3,4], Nadine Ebert‡[2,3], Donata Hoffmann‡[1], Martin Beer‡[1,5], Volker Thiel‡[2,3,4,5]

Affiliations:

[1] Institute of Diagnostic Virology, Friedrich-Loeffler-Institut, Greifswald-Insel Riems, Germany
[2] Institute of Virology and Immunology, Bern and Mittelhäusern, Switzerland
[3] Department of Infectious Diseases and Pathobiology, Vetsuisse Faculty, University of Bern, Bern, Switzerland
[4] Multidisciplinary Center for Infectious Diseases, University of Bern, Bern, Switzerland
[5] European Virus Bioinformatics Center, Jena, Germany
[6] Department of Experimental Animal Facilities and Biorisk Management, Friedrich-Loeffler-Institut, Greifswald-Insel Riems, Germany
[7] Graduate School for Cellular and Biomedical Sciences, University of Bern, Bern, Switzerland
[8] COMPATH, Institute of Animal Pathology,,University of Bern, Bern, Switzerland
[9] Institute of Veterinary Bacteriology, Department of Infectious Diseases and Pathobiology, Vetsuisse Faculty, University of Bern, Bern, Switzerland.
[10] RocketVax AG; 4057 Basel, Switzerland

†These authors contributed equally to this work.
‡These authors jointly lead this work.

*Corresponding authors.
Volker Thiel; e-mail: volker.thiel@vetsuisse.unibe.ch; phone: +41-31-6312413
Martin Beer; e-mail: martin.beer@fli.de; phone: +49-38-35171200

Abstract

Vaccines are the most effective measure against COVID-19. However, novel and highly efficacious vaccines with simplified administration and broad immunogenicity, providing systemic and mucosal immunity are needed. Here, we show the development of live-attenuated vaccines (LAV) based on (i) recoding the SARS-CoV-2 genome to enrich for "one-to-stop" (OTS) codons, (ii) facilitating host responses by disabling non-structural-protein-1 (Nsp1) mediated translational repression, and deletion of open reading frames (ORF) 6, 7ab and 8, and (iii) deleting the spike polybasic cleavage site (PCS) to reduce LAV replication in the lung and prevent vaccine shedding. The OTS-modified SARS-CoV-2 LAV is adjustable regarding the level of attenuation, particularly vulnerable to mutagenic antiviral drugs, and protects efficiently against wild-type (WT) SARS-CoV-2 and recent variants of concern (VOC) in K18-hACE2 transgenic mice and Syrian hamsters. Furthermore, LAV immunization results in faster virus clearance after SARS-CoV-2 challenge compared to mRNA vaccines, a complete block of transmission of WT SARS-CoV-2, and significantly reduced transmission of Omicron BA.2 and BA.5 variants. Overall, the newly developed OTS-based LAVs represent a new generation of live vaccines that are intranasal administered at the natural site of infection, provide efficient and innovative infection control, and conceptionally are readily applicable to many other emerging viruses.

Main

The emergence of the severe acute respiratory syndrome coronavirus 2 (SARS-CoV-2) in 2019 led to global spread and the evolution of various concerning virus variants[1]. Despite the rapid development of mRNA and viral vector-based vaccines, the currently approved vaccines primarily target the spike protein antigen, providing limited protection against infection with novel virus variants and viral transmission. Consequently, SARS-CoV-2 can evade immunity through spike gene mutations, hindering consistent interruption of infection chains[1]. Therefore,

there is an urgent need for more robust vaccination strategies that generate broad immunogenicity.

To address these challenges, we present the development and characterization of a new type of SARS-CoV-2 live attenuated vaccines (LAVs) based on the one-to-stop (OTS) approach. This technique takes advantage of the natural error rate of RNA virus polymerases to attenuate the virus[2]. By introducing synonymous codon changes into the open reading frame (ORF) 1ab, we maintained identical amino acid sequences to the wild-type virus while increasing the probability that premature termination codons will appear. This compromises viral fitness and pathogenicity, contributing to attenuation.

To enhance safety and antigenicity, we also mutated non-structural protein 1 (Nsp1) and deleted specific ORFs, including ORFs 6 to 8, and the polybasic spike S1/S2 cleavage site (PCS). Nsp1 proteins inhibit cellular mRNA translation, so eliminating this function facilitates viral attenuation[3]. Accessory proteins encoded by ORFs 6, 7a, 7b, and 8 are associated with immune evasion mechanisms, including interference with interferon-stimulated genes and antigen presentation[4-7]. By deleting these ORFs, we aim to promote early interferon responses, enhance LAV attenuation, and improve immunogenicity[8-11]. Furthermore, we removed the PRRAR motif from the PCS, as it has been implicated in transmission efficiency and attenuation[12-14].

We generated several vaccine candidates using the OTS approach, and their attenuation levels were adjustable based on the extent of genome modification. Enriching OTS codons increased vulnerability to mutagenic drugs. The combination of Nsp1 (K164A/H165A) mutations and ORF6-8 knockout resulted in a fully protective LAV candidate named OTS-206 against severe disease from various virus variants. Additionally, LAV candidate OTS-228, which included an extra deletion of the PCS, successfully blocked LAV transmission without compromising its protective capacity.

Through *in vitro* and pre-clinical animal model assessments using K18-hACE2 mice and Syrian hamsters, we demonstrated that our LAV candidates possess exceptional safety profiles, while inducing long term protective immunity. They induce sterile immunity against the original SARS-CoV-2 strain as well as full protection and reduced transmission against recent variants such as Omicron BA.2 and BA.5.

In summary, our novel LAV candidates based on the OTS approach offer solutions for a robust and adaptable SARS-CoV-2 vaccination strategy. They are easy to apply, elicit strong protective immune responses, prevent severe disease, and reduce viral shedding and breakthrough infections. The exceptional safety profile and efficacy of these candidates position them as alternatives to current mRNA vaccines.

Development of novel SARS-CoV-2 live attenuated vaccine (LAV) candidates using the one-to-stop (OTS) approach

To incorporate OTS modifications into the SARS-CoV-2 genome, we used the in-yeast transformation-associated recombination (TAR) cloning method[15]. Nucleotide changes were introduced to specific areas of ORF1ab targeting serine and leucine codons (**Fig. 1a**). Specifically, we changed serine and leucine codons that can become stop codons by two mutations to synonymous codons that require only one mutation to become a stop codon. This resulted in various recombinant SARS-CoV-2 mutants: OTS2, OTS4, OTS5, OTS7, and OTS8 (**Fig. 1a**, **Extended Data Fig. 1a**, **Supplementary Table 1**). We combined these recoded fragments to create OTS4-5, OTS7-8, and finally OTS4-5-7-8 mutants. The OTS4-5-7-8 mutant had a total of 576 mutations and 325 synonymous codon changes in the recoded ORF1ab (**Supplementary Table 1**).

For the subsequent OTS live attenuated vaccine (LAV) candidates, we used the most extensively recoded ORF1ab from OTS4-5-7-8 as the foundation. The OTS-206 vaccine virus

111 combined the OTS4-5-7-8 mutations with two amino acid substitutions (K164A, H165A) in the
112 Nsp1 gene and the deletion of the accessory genes ORF6-8 (**Fig. 1a**). To create the final LAV
113 candidate, OTS-228, we deleted the polybasic spike S1/S2 cleavage site (ΔPRRAR) from OTS-
114 206 (**Fig. 1a**).

115 **OTS constructs are more sensitive to treatment with mutagenic drugs, but show *in vitro***
116 **replication kinetics comparable to SARS-CoV-2 WT**

117 We compared plaque sizes and replication kinetics of different OTS viruses to the ancestral
118 wild-type SARS-CoV-2 (WT) to evaluate the impact of OTS changes. OTS4-5, OTS7-8, OTS4-
119 5-7-8, and OTS-206 exhibited great variation in plaque sizes on VeroE6 cells. On average,
120 OTS4-5, OTS7-8, and OTS-206 had smaller plaques, though not statistically significant, while
121 OTS4-5-7-8 had larger plaques (**Fig. 1b, Extended Fig. 1b**).

122 We assessed viral replication kinetics in VeroE6/TMPRSS2 cells, human nasal epithelial cells
123 (hNECs), and bronchial epithelial cells (hBECs). OTS4-5, OTS7-8, OTS4-5-7-8, and OTS-206
124 replicated similarly to WT in VeroE6/TMPRSS2 cells but displayed notable differences in
125 hNECs and hBECs (**Fig. 1c-e, Extended Data Fig. 1c,d**). In hNECs, OTS4-5-7-8 and OTS-
126 206 exhibited reduced fitness compared to WT, with lower apical titers up to 96 hours post-
127 infection (hpi) (**Fig. 1d**). Variability was observed in hBECs for OTS4-5, OTS7-8, and OTS4-
128 5-7-8, while OTS-206 reached similar titers as WT at 96 hpi (**Fig. 1e**). Recombinant viruses
129 with Nsp1 mutation (K164A, H165A) or deletion of accessory ORFs 6-8 (delORF6-8) served
130 as controls for OTS-206 (**Extended Data Fig. 1c,d**). The Nsp1 mutant displayed kinetics
131 similar to WT in both the cell line and hBECs, while the delORF6-8 virus showed increased
132 titers at 24 hpi in VeroE6/TMPRSS2 and 96 hpi in hBECs (**Extended Data Fig. 1c,d**).

133 Furthermore, we assessed the vulnerability of OTS4-5-7-8 to 5-fluorouracil (5-FU) and
134 molnupiravir treatment, expecting increased susceptibility due to OTS modifications. OTS4-5-

7-8 showed a dose-dependent decrease in viral titers compared to WT when exposed to 5-FU (**Fig. 1f**). Although not as dramatic as with 5-FU, OTS4-5-7-8 replicated significantly less than WT when treated with molnupiravir (**Fig. 1g**).

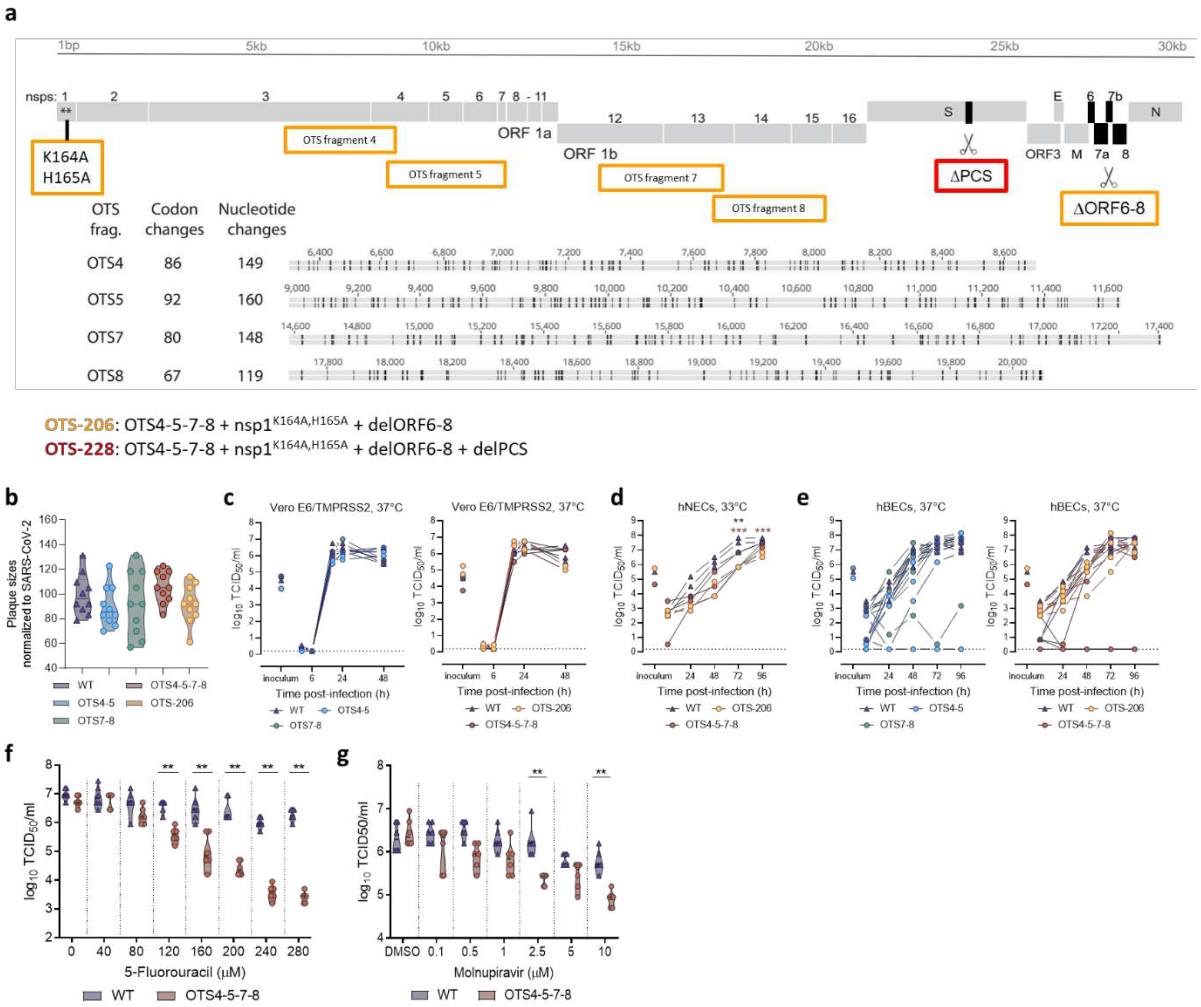

Fig. 1. OTS constructs exhibit similar replication kinetics to WT in vitro, but are more sensitive to mutagenic drugs. a, Overview of mutations introduced to SARS-CoV-2 genome to generate live-attenuated vaccines. Fragments 4, 5, 7, and 8 were modified to generate one-to-stop codons. Specific changes are indicated for each fragment. OTS-206 also has additional Nsp1 mutations (K164A/H165A) and deletions from ORF6 to ORF8. OTS-228 lacks the PCS in addition. **b,** Comparable plaque sizes between OTS and WT^{D614G} viruses. No significant difference found using ordinary one-way ANOVA and p-values were adjusted using Tukey's multiple-comparison test. **c,** Infection of Vero E6/TMPRSS2 cells and **d,** human nasal (hNECs) and **e,** bronchial epithelial cells (hBECs) with WT and OTS viruses. Samples collected at designated time points for infectious particle titer assessment. Statistical analysis performed using two-way ANOVA. **f,** and **g,** Treatment of Vero E6/TMPRSS2 cells with 5-Fluorouracil (5-FU) and Molnupiravir, followed by infection with WT or OTS4-5-7-8, indicating a higher sensitivity of OTS-4-5-7-9 to 5-FU and Molnupiravir. Additional data in **Extended Data Fig.1**. Statistical significance was assessed by unpaired, nonparametric multiple t-test with Mann-Whitney test (compared ranks). No asterisk indicates no statistical significance. *P<0.05, **P < 0.01, ***P<0.001, ****P<0.0001.

Stability of OTS modifications

The genetic stability of OTS4-5, OTS7-8, OTS-228, and WT SARS-CoV-2 after ten or fifteen passages in VeroE6 cells was assessed by next-generation sequencing (NGS). WT SARS-CoV-2 was passaged fifteen times in VeroE6 cells as a control. OTS4-5, OTS7-8, and WT exhibited loss of the S1/S2 cleavage site through deletion (S 679-NSPRRAR-685), a known characteristic when SARS-CoV-2 is propagated in TMPRSS2-deficient environments like VeroE6 cells[16]. However, the S1/S2 cleavage site of OTS-206 and the PRRAR deletion of OTS-228 remained unchanged when passaged on VeroE6/TMPRSS2 cells (**Supplementary Table 5**).

Crucially, none of the modified leucine and serine codons (OTS codons) reverted to the wild-type sequence after ten passages (OTS4-5, OTS7-8, and OTS-206) or fifteen passages (OTS-228) in either VeroE6 or VeroE6/TMPRSS2 cells. Additionally, the introduced Nsp1 mutations (K164A, H165A) in OTS-206 and OTS-228, as well as the ORF6-8 deletions, were retained during passage.

Fine-tuning OTS genome modification influences attenuation levels

To assess the attenuation levels of OTS mutations, various experiments were conducted in K18-hACE2 mice and Syrian hamsters (**Extended Data Fig. 2a**). In K18-hACE2 mice, individual OTS mutations (OTS2, OTS7, OTS8) resulted in no weight loss (**Extended Data Fig. 2b)** or clinical signs (**Extended Data Fig. 2c**). Nevertheless infectious virus titers (**Extended Data Fig. 2d**), genome copies (**Extended Data Fig. 2e**), and lung pathology (**Extended Data Fig. 2f,g**) were comparable to WT, but no detectable infectious virus progeny was found with OTS2 and OTS7 in the nasal conchae or OTS7 in the brain (**Extended Data Fig. 2d**). Therefore, aiming for greater attenuation, OTS mutations in multiple fragments (OTS4-5, OTS7-8) (**Extended Data Fig. 2h**) and the OTS-206 construct, which included Nsp1 mutations and ORF6-8 knockout, were tested.

In K18-hACE2 mice, WT SARS-CoV-2 inoculated and one of the OTS4-5 inoculated mice were associated with weight loss (**Extended Data Fig. 2i**), while only WT exhibit clinical signs 5 days post inoculation (dpi) (**Extended Data Fig. 2j**). Infectious virus titers in the lungs, noses, and brains of OTS4-5 and OTS7-8 infected mice were lower than WT, or even completely negative for OTS7-8 nose and brain samples (**Extended Data Fig. 2k**), although viral RNA copies were still high (**Extended Data Fig. 2l,m)**. Notably, none or very low levels of viral N protein was detected immunohistochemically in the brains of mice immunized with OTS constructs (**Extended Data Fig. 2g,o**). In addition, we compared OTS4-5, OTS7-8, and OTS-206 to WT in the Syrian hamster model (**Extended Data Fig. 3a**). While none of the OTS constructs induced lethality, OTS4-5 and OTS7-8 caused weight loss similar to WT, which was not observed with OTS-206 (**Extended Data Fig. 3b**). OTS-206 also showed reduced genome copy numbers in nasal washings (**Extended Data Fig. 3d**) and respiratory tract tissues compared to OTS4-5 and OTS7-8 (**Extended Data Fig. 3f,g**). Histopathology revealed SARS-CoV-2 characteristic lung lesions, virus antigen was consistently found in all animals, predominantly in type I pneumocytes (**Extended Data Fig. 3k,l**).

Transmission was observed for OTS4-5 and OTS7-8 inoculated hamsters to naïve contact animals. Respective contact hamsters experienced weight loss, while OTS-206 contact animals did not (**Extended Data Fig. 3c**). Viral RNA copies in nasal washings (**Extended Data Fig. 3d, e**) and organs (**Extended Data Fig. 3h**) and seropositivity (**Extended Data Fig. 3i,j**) were detected in contact animals, confirming transmission. Importantly, sequencing of 21 dpi conchae samples of OTS4-5 and OTS7-8 contact animals confirmed that the OTS codons remained stable after *in vivo* passage (**Supplementary Figure 5**).

In summary, introducing OTS codon modifications in two combinations (OTS4-5 and OTS7-8) led to modest attenuation in K18-hACE2 mice and Syrian hamsters, reducing virulence but not eliminating weight loss or viral shedding. However, when four genome fragments were

recoded in the OTS-206 construct, significant attenuation was observed, with no weight loss and restricted viral replication in URT and LRT. While no clinical signs were observed, some lung lesions were still present, but the OTS genome modifications remained genetically stable after *in vivo* passage.

Immunization with OTS constructs lead to full protection against SARS-CoV-2 challenge infection

To evaluate the immunogenicity and protective efficacy of OTS4-5-7-8 and OTS-206 compared to OTS4-5 and OTS7-8, we conducted intranasal immunization of K18-hACE2 mice (**Fig. 2a, Extended Data Fig. 4a)**. Mice immunized with OTS4-5-7-8 and OTS-206 showed no significant weight loss or clinical symptoms pre-challenge (**Extended Data Fig. 4b,c**), unlike half of the animals immunized with OTS4-5 or OTS7-8, which reached end-point criteria and were euthanized (**Fig. 2b,c**). At 21 days post immunization, all mice were challenged with WT SARS-CoV-2. Naïve mice in the control group reached a humane endpoint and had to be euthanized 5- or 6-days post-challenge (**Fig. 2d,e,f**), while mice immunized with OTS4-5 and OTS7-8 displayed rapid recovery and no significant weight loss or clinical signs post-challenge **(Fig. 2d,e,f**). The viral genome copies in the nose and lung samples of OTS-immunized mice were significantly lower than those of non-immunized mice (**Fig. g, h, Extended Data Fig. 4e-h**). No infectious virus was detected in the samples of pre-immunized and challenged mice, indicating virus clearance (**Fig 2i, Extended Data Fig. 4d,f**). Histopathological analysis showed mild lung leukocytic infiltrates with follicle formation in mice immunized with OTS4-5, while mice immunized with OTS4-5-7-8 showed moderate to severe lung pathology (**Extended Data Fig. 4i**). However, mice pre-immunized with OTS-206 exhibited only minor signs of infection that resolved quickly (**Extended Data Fig. 4i**). These findings confirmed that the OTS LAV candidates provided protection against lethal SARS-CoV-2 challenge and

224 elicited neutralizing antibody responses (**Extended Data Fig. 4j**) and SARS-CoV-2 spike-
225 specific CD8 T-cell responses (**Extended Data Fig. 4k**).

226 The protective efficacy of OTS LAV was further evaluated in Syrian hamsters. In the first
227 experiment, hamsters were immunized with OTS4-5 or OTS7-8 and challenged with WT
228 SARS-CoV-2 (**Fig. 2l**). None of the immunized hamsters succumbed to the challenge infection,
229 while three out of four naïve control animals did (**Fig. 2m**). The immunized animals did not
230 experience weight loss, in contrast to the control group (**Fig. 2n**). Viral genome copy numbers
231 in nasal washing samples were significantly lower in the immunized groups (**Fig. 2o**). At 14
232 days post-challenge, viral genome loads in organ samples were barely above the threshold,
233 indicating virus clearance (**Fig. 2p**). However, transmission of the challenge virus to naïve
234 contact animals was not blocked by OTS4-5 or OTS7-8 immunization, as proven by increased
235 lethality (**Fig. 2m)**, body weight loss (**Fig. 2n**), virus genome positive nasal washing (**Fig. 2o**)
236 and organ samples (**Fig. 2p**), as well as serological evaluation of the final serum samples
237 (**Extended Data Fig. 4l,m**).

238 In the second experiment, hamsters were immunized with OTS-206 and challenged with the
239 SARS-CoV-2 Omicron BA.2 variant (**Fig. 2q**). Neither the immunized nor the naïve hamsters
240 in direct contact showed any lethality (**Fig. 2r**), or weight loss, while the challenged naïve
241 control animals continuously lost weight (**Fig. 2s**). Viral RNA in nasal washing samples was
242 significantly reduced in the immunized group compared to the control group (**Fig. 2t**), and
243 delayed virus transmission to contact animals for the immunized group (**Fig. 2t**). Analysis of
244 organ samples showed high protection against BA.2 replication in the lung of OTS-206-
245 immunized animals (**Fig. 2u, Extended Fig. 4n**). Sera from OTS-206-immunized hamsters
246 exhibited a high level of wild type RBD-specific antibodies (**Extended Fig. 4o**) and
247 neutralizing capacity against both WT^{D614G} and Omicron BA.2 (**Extended Fig. 4p**). Although
248 transmission of the challenge virus to direct contact animals could not be prevented, OTS-206-

immunized hamsters were protected from weight loss, and pulmonary atelectasis (**Extended Data Fig. 4 q,r**), with only marginal virus antigen detectable in lung samples (**Extended Data Fig. 4 s,t**).

In conclusion, immunization with OTS LAV candidates provided protection against lethal SARS-CoV-2 variant challenge in mice and hamsters. The vaccines elicited neutralizing antibody responses and specific CD8 T-cell responses. While OTS4-5 and OTS7-8 reduced viral loads and prevented lethality and morbidity in hamsters, they did not block transmission to naïve contact animals. OTS-206 immunization showed superior protection against weight loss, pulmonary atelectasis, and viral replication, but transmission to contact animals still occurred.

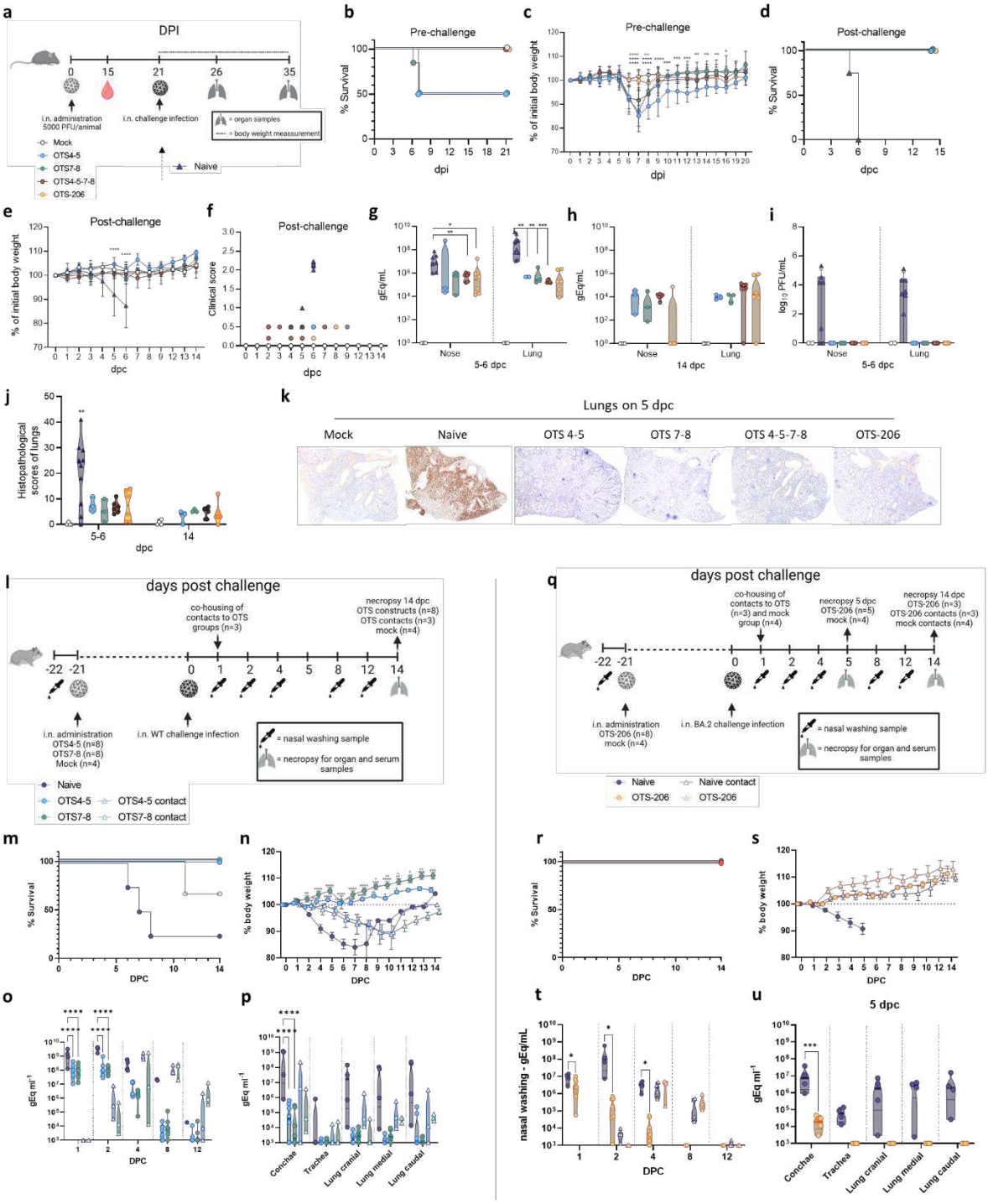

Fig. 2: Immunization with OTS constructs provides full protection against SARS-CoV-2 challenge. a, Intranasal inoculation of K18-hACE2 mice (n=12 mice/group) with OTS4-5, OTS7-8, OTS4-5-7-8, and OTS-206 and subsequent challenge with WT SARS-CoV-2 at 21 days post-inoculation (dpi), including a naïve challenge control group. **b,** Pre-challenge survival (%) and **c,** body weight loss shows a correlation between increased OTS modifications and improved outcomes. All OTS constructs provide full protection against challenge infection in terms of **d,** survival and **e,** body weight. **f,** Clinical scores post-challenge are high only in naïve mice. **g, h,** Viral genome copies in nose and lung samples are significantly reduced for the vaccinated animals, **i,** while already 5-6 days post challenge (dpc) no infectious virus was detectable in nose and lung samples of the vaccinated ones. **j,** Histopathological scores and **k,** immunohistochemical analysis of lung sections demonstrate protection in OTS-construct-inoculated mice. **l,** Syrian hamsters inoculated with OTS4-5 or OTS7-8, and subsequently challenged, exhibit **m,** survival and **n,** weight stability post challenge, with **o,** reduced viral genome copies in nasal washings and **p,** respiratory tissues. Similar results are observed in **q,** hamsters inoculated with OTS-206 and challenged with BA.2 VOC.

r, Challenged hamsters do not exhibit any mortality and **s,** vaccinated ones were protected from weight loss. **t,** Also shedding of virus genome was significantly reduced, **u,** as well as in Conchae samples and even complete absent in all lung samples examined. More data is presented in **Extended Data Fig.3** and **Extended Data Fig.4**. Statistical significance of differences were determined by ordinary one-way ANOVA (panels **g, h,** and **j,**) or two-way ANOVA ((Tukey's multiple comparison test (panels **o,** and **p,**)) or (uncorrected Fisher´s LSD (panels **t,** and **u,**)), individual variances computed for each comparison were used. No asterisk indicates no statistical significance. *P<0.05, **P-<-0.01, ***P<0.001, ****P<0.0001.

OTS-206 induces long-term immunity, shows comparable efficacy to mRNA-vaccines, but is superior in virus clearance after challenge infection

We challenged K18-hACE2 mice 28 days after they were immunized with a single dose of a mRNA-vaccine (monovalent Spikevax) or the OTS-206, with SARS-CoV-2 VOC Delta (B.1.617.2) (**Fig. 3a**). To assess vaccine protection early after challenge infection, lungs were harvested 2- or 5 dpc. Immunohistochemistry of the whole lungs showed a variable but higher abundance of nucleocapsid proteins detected in mRNA vaccinated mice 2 dpc, and was almost undetectable in both conditions 5 dpc (**Fig. 3b,c**). Spatial transcriptomics of the lungs focusing on SARS-CoV-2 transcripts confirmed lung immunohistochemistry results and showed higher viral mRNA expression per capture spot in the lung tissue for the mRNA vaccinated mice than for the OTS-206 vaccinated mice (**Fig. 3d**). Strikingly, different SARS-CoV-2 transcripts were detected at lower levels in OTS-206 vaccinated mice at 2 dpc compared to mRNA-vaccinated mice, and not detected anymore at 5 dpc in OTS-206 vaccinated mice (**Fig. 3d,e**), suggesting faster clearance of the challenge virus in OTS-206 vaccinated mice. We also assessed spatial host gene transcriptional expression in the vicinity of sites of virus infection in the lungs. We compared the pathway activity scores constructed from the expression changes of the top 100 genes that are involved in several cellular pathways such as MAPK, JAK-STAT, TGF-β and TNF-α (**Fig. 3f**). We observed a consistent spatial correlation pattern between the viral and the host genes in the infected lungs for the mRNA and OTS-206 groups 2 dpc (**Extended Data Fig. 5a**). This similarity in gene expression signatures suggests a comparable response in terms of gene activation between the two conditions. It is interesting to note that the mRNA and OTS-206 groups share 8 of the 20 host genes with the highest spatial correlation with virus RNA

transcripts (**Extended Data Fig. 5b**). The expression of pro-inflammatory cytokines that have been reported to be upregulated in SARS-CoV-2 patients[17,18] was elevated in the mRNA vaccinated group compared to the OTS-206 group (**Extended data Fig. 5c**). Notably, the JAK-STAT pathway, that is crucial in processes such as innate and adaptive immune responses, cell division, hematopoiesis and tissue repair, showed significantly increased activity in the lung at sites of infection (**Extended data Fig. 5d**). As shown in the violin plots, which show the underlying distribution of pathway scores in each capture spot, the JAK-STAT pathway activation at 2 dpc was higher in mRNA-vaccinated mice compared to OTS-206 vaccinated mice (**Fig. 3f**). Most strikingly, at 5 dpc, JAK-STAT activation was almost back to baseline levels in OTS-206 vaccinated mice. These results demonstrate that faster clearance of heterologous SARS-CoV-2 VOC Delta is accompanied by faster resolution of virus-induced host responses in K18-hACE2 mice. We then immunized K18-hACE2 mice either with a homologous or heterologous prime-boost combination of mRNA vaccine (monovalent Spikevax) or OTS-206. To compare the immediate protection, mice were challenged with WT^{D614G} or the Delta VOC (B.1.617.2) 28-days post-boost (28 dpb), while long term protection was evaluated by challenge 5 months post-boost (5 mpb) using the WT^{D614G} virus (**Fig. 3g, Extended data Fig. 6a, b**). All immunized mice, regardless of the immunization combination or the challenge virus, were protected from disease and body weight loss, when challenged 28 days post-boost or 5 months post-boost (**Fig. 3h,k**). No infectious virus was detected 6 dpc in nose or lung samples of the immunized animals (**Fig. 3i,l**). Naïve WT^{D614G} and Delta VOC challenged mice showed similar levels of viral titers (**Fig. 3i**), but the histopathological score of the lungs of Delta-challenged mice was significantly higher than the histopathological lung scores of WT^{D614G}-challenged mice (**Fig. 3j**). Viral RNA load in organ samples and oropharyngeal swabs of all immunized groups showed a significant reduction in replication compared to the naïve control animals which were challenged with either WT or Delta VOC (**Extended data Fig. 6c**). Strikingly, mice challenged 5 months post-boost showed less amount

of viral RNA in the organ samples compared to the similarly immunized mice challenged 57 days post prime immunization (**Extended data Fig. 6e**), pointing that the protection provided by the immunization did not decrease within 5 months. This trend was also reflected in the histopathological scores of the lungs (**Fig. 3j,m**). Altogether, these data show the ability of OTS-206 to induce long-term protection against SARS-CoV-2 in the very sensitive K18-hACE2 mice model equally to an established mRNA-vaccine.

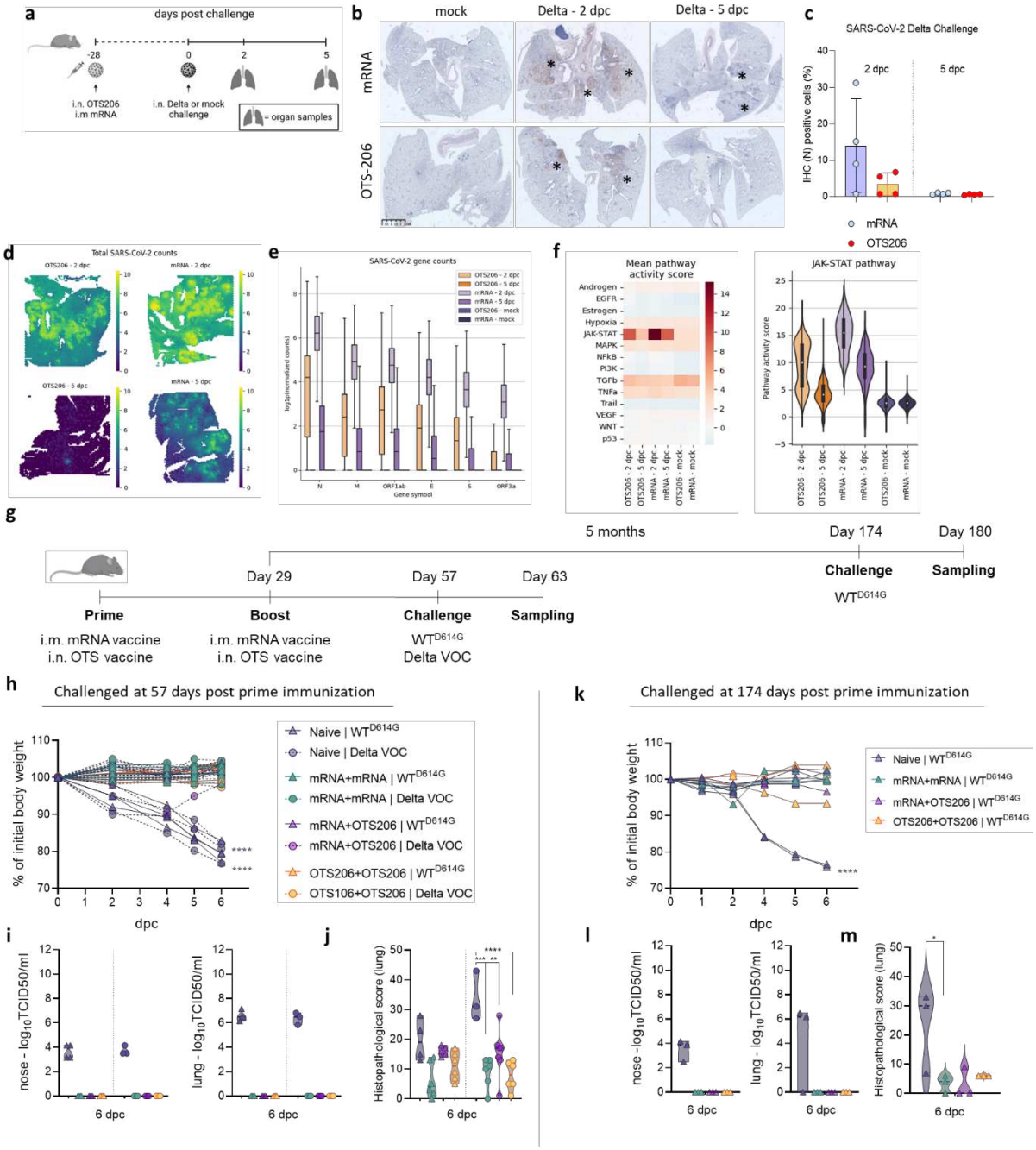

Fig. 3: OTS-206 induces long-term immunity, comparable efficacy to mRNA-vaccines, superior virus clearance after challenge infection. a, Short term experimental setup: K18-hACE2 mice vaccinated with Spikevax mRNA-vaccine (intramuscularly) or OTS-206 (intranasally) (n=8 mice/group). Challenge with SARS-CoV-2 Delta VOC, lung harvest at 2- or 5-days post challenge (dpc). **b,** Immunohistochemistry of lung sections for SARS-CoV-2 nucleocapsid protein. **c,** Quantification of nucleocapsid-stained lung cells. **d, e,** Summed and normalized SARS-CoV-2 gene counts (N, ORF1ab, M, E, S, ORF3a). Both, IHC and gene count quantification, indicating faster clearance of SARS-CoV-2 for the OTS-206 group than for the mRNA group. **f,** Increased JAK-STAT pathway activity post challenge, highest activity for mRNA-group 2 dpc. **g,** Long term experimental setup: K18-hACE2 mice were prime-boost immunized with Spikevax or OTS-206 or a combination. Challenge infection with WT^{D614G} or SARS-CoV-2 Delta VOC either 57 days post prime immunization or 5 months post prime immunization (n=8 mice/group). **h, k,** Independently of the time point of challenge, none of the vaccinated animals lost body weight, **i, l,** nor does any of the vaccinated animals exhibit infectious virus in nose and lung samples 6 dpc, indicating good clinical long-term protection. **j, m,** High level of long-term protection was confirmed by histopathological scores for lung pathology. Statistical significance determined using ANOVA. Data obtained from one experiment. Infectious viral particle concentrations, genome copies, and immunohistochemical analysis in **Extended Data Figure 6**. Body weight changes, clinical scores, and histopathological scores in **Supplementary Table 6**. Statistical significance was determined using two-way ANOVA (Tukey's multiple comparison test) (panels **h,** and **k,**) or ordinary one-way ANOVA (panels **j,** and **m,**). No asterisk indicates no statistical significance. *P<0.05, **P<0.01, ***P<0.001, ****P<0.0001.

Deletion of the spike polybasic cleavage site blocks LAV transmission, and inhibits transmission of WT SARS-CoV-2 challenge infections

The OTS-206 vaccine, although well-attenuated and effective in providing immunity against different variants of SARS-CoV-2, had a drawback of being transmitted to contacts. To address this, we developed an improved version called OTS-228 by removing the polybasic cleavage site (PCS) in the spike protein (**Fig. 4a**).

In vitro analysis showed that the deletion of the PCS resulted in smaller plaque sizes (**Fig 4b**), no impaired replication in VeroE6/TMPRSS2 cells (**Extended Data Fig. 7**), but delayed replication kinetics in human nasal epithelial cells (hNECs), and reduced viral titers in human bronchial epithelial cells (hBECs) (**Fig 4c**). The transmissive potential of OTS-228 was evaluated in a hamster model. Ten hamsters were intranasally inoculated with OTS-228, and four naïve contact animals were introduced at 1-day post-inoculation (**Fig. 4d**). None of the inoculated animals or contact animals experienced lethality (**Fig. 4e**) or weight loss (**Fig. 4f**). While the viral genome was detectable in nasal washing samples of the inoculated hamsters until 7 days post-inoculation to levels of 10^7 gEq/mL and higher, contact animals exhibited only marginal amount of virus genome at two time points (3399 (3 dpi) and 1782 (4 dpi) gc/mL) (**Fig. 4g**). The viral RNA in samples collected from the inoculated animals at 5 days post-inoculation showed a significant reduction, except in the conchae organ samples, where viral

genome was still detectable at 21 days post-inoculation **(Fig 4h)**. The genetic stability of the OTS-228 modifications was confirmed through deep sequencing of these conchae samples (**Supplementary Data Table 1**). No viral genome was detected in organ samples from the naïve contact animals at 21 days post-inoculation **(Fig 4h)**. Serological evaluation confirmed that all contact animals remained seronegative after 20 days of direct contact with the inoculated hamsters **(Fig 4i)**. The immunized animals showed neutralizing capacity against WT SARS-CoV-2, while one animal even exhibited neutralizing activity against the Omicron BA.2 and BA.5 variants (**Fig. 4j**). Histopathological analysis of the lungs from the inoculated hamsters at 5 days post-inoculation showed no signs of pneumonia-related atelectasis or characteristic SARS-CoV-2 vascular or bronchial lesions (**Supplementary Fig. 2a-d**). Some animals exhibited mild expansion of the pulmonary interstitium with macrophages, and a focal perivascular immune cell infiltration was found in one hamster.

These findings demonstrate that OTS-228 is completely attenuated and capable of inducing a broad neutralizing humoral immune response in the Syrian hamster model. Most importantly, transmission to naïve direct contact animals was completely prevented, addressing a key concern associated with the previous OTS-206 vaccine candidate.

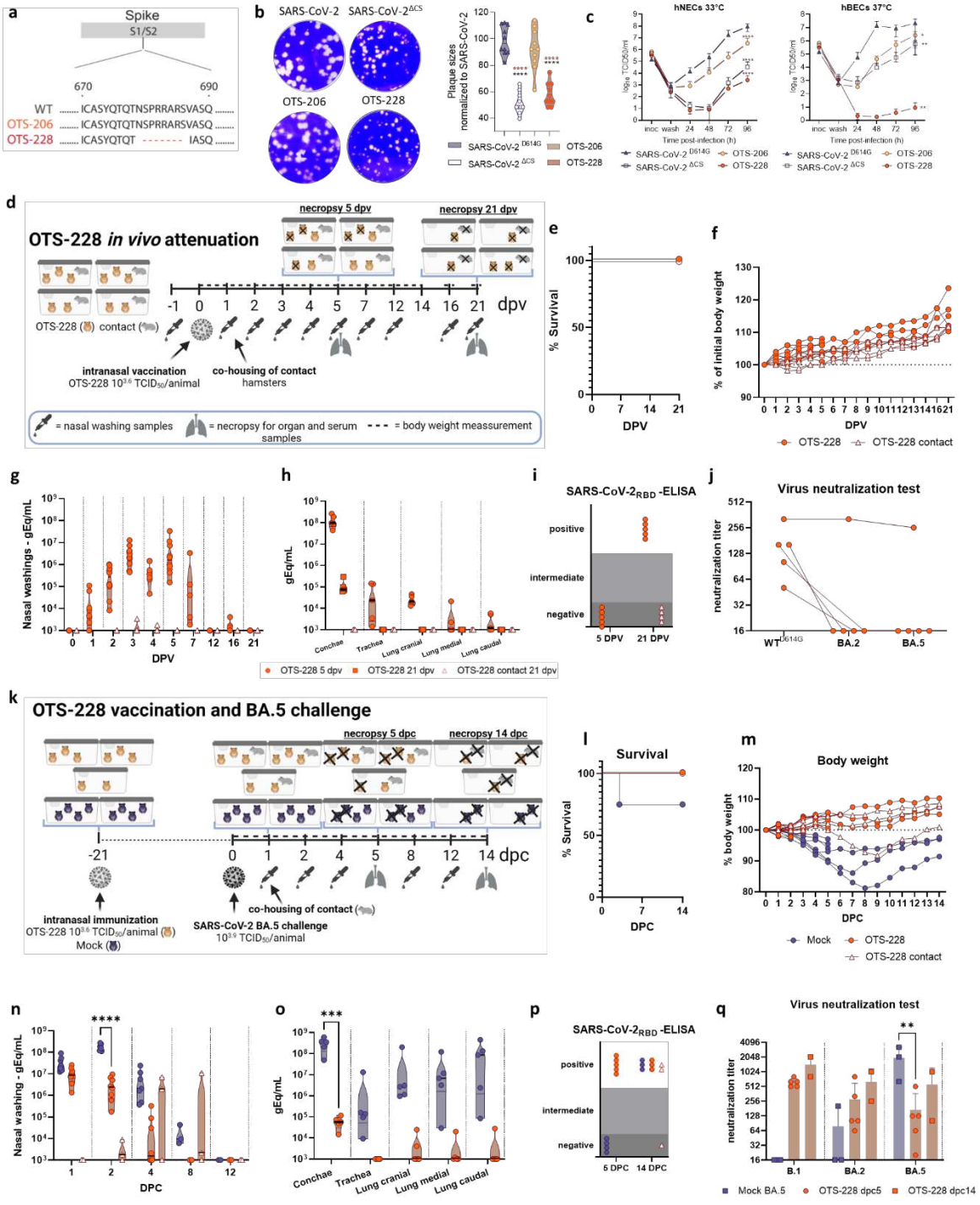

Fig. 4: OTS-228 significantly reduces transmission, protects against, and limits transmission of SARS-CoV-2 VOC challenge infections. a, Schematic representation of the deleted polybasic cleavage site in OTS-228 spike region compared to WT and OTS-206. **b,** Reduced plaque sizes observed with CS deletion. **c,** Infection of human nasal (hNECs) and bronchial epithelial cells (hBECs) with indicated viruses. Infectious particle titers assessed over time, confirming attenuation OTS-228 in both cell lines. **d,** Attenuation experiment in Syrian hamsters with OTS-228. **e,** Full attenuation of OTS-228 in terms of survival and **f,** body weight changes of vaccinated and contact hamsters. **g,** OTS-228 genome was not transmitted to naïve direct contact hamsters, beside **h,** high genome loads in Conchae samples at 5 days post vaccination (dpv). **i,** Analyzed serum samples confirmed lack on transmission to contacts and **j,** highlighting a partly humoral cross variant neutralizing immune response. **k,** Omicron BA.5 challenge infection of OTS-228-vaccinated Syrian hamsters. **l,** Mortality and **m,** body weight loss was prevented by OTS-228 vaccination. **n,** Shedding of Omicron BA.5 virus genome was significantly reduced **o,** and accordingly so in the Conchae samples, while Omicron BA.5 was nearly absent in lung samples 5 dpc. **p,** Serological evaluation confirmed reduced transmission to naïve contact animals. **q,** Evaluating the post-challenge humoral immune response, showed

broad neutralization capacity of OTS-228 against WT^{D614G}, but also against Omicron BA.2 and BA.5, while control sera only reacts against Omicron BA.5. Statistical significance was determined using two-way ANOVA and p-values were adjusted using Tukey's multiple comparison test; *P<0.05, **P<0.01, ***P<0.001, ****P<0.0001.

OTS-228 vaccination protects against VOC challenge infection and limits challenge virus transmission events

We assessed the protective efficacy of the OTS-228 vaccine against WT SARS-CoV-2 (**Extended Data Fig. 8a**), but also against recent variants of concern (VOCs), such as Omicron BA.2 (**Extended Data Fig. 9a**) and Omicron BA.5 (**Fig. 4k**). These immunized and challenged animals were co-housed with non-immunized contact animals.

Remarkably, OTS-228 immunization resulted in full protection against lethality (**Extended Data Fig. 8b**) and body weight loss (**Extended Data Fig. 8c**), significantly reduced shedding of viral genome (**Extended Data Fig. 8d**) and drastically reduced genome loads in organ samples (**Extended Data Fig. 8e,f)**. In turn, virus transmission of the WT virus to naïve contact animals was prevented (triangles in **Extended Data Fig. 8b,c,d,f**), also corroborated by serology (**Extended Data Fig. 8g,h**).

After the Omicron BA.2 challenge, no lethality (**Extended Data Fig. 9b**) or weight loss was observed (**Extended Data Fig. 9c)**. Virus shedding (**Extended Data Fig. 9d**) and replication in the lungs was significantly reduced (**Extended Data Fig. 9e**), and no viral genome was detected at 14 days post-challenge (**Extended Data Fig. 9f**). Among the contact animals, only one showed evidence of infection through serological analysis (**Extended Data Fig. 9g)**. The immunized animals exhibited similar neutralizing titers against both the WT^{D614G} and the Omicron BA.2 variant (**Extended Data Fig. 9h**).

Following Omicron BA.5 challenge, the OTS-228-immunized animals did not experience lethality or weight loss in contrast to the control animals, and one control animal unfortunately did not regain consciousness after the brief anesthesia, passed away during the sampling

procedure (**Fig. 4l,m**). Viral loads in the nasal washing samples of the immunized group were significantly lower compared to the non-immunized group (**Fig. 4n**). By 8 days post-challenge, the immunized animals had undetectable levels of viral genome in nasal washing samples, while the non-immunized mock animals still showed viral presence (**Fig. 4n**). Viral loads in organ samples and conchae were also significantly reduced in the immunized animals (**Fig. 4o)**. All lung samples from the immunized animals tested negative for the virus at 14 days post-challenge (**Extended Data Fig. 10**). Serological evaluation confirmed the presence of SARS-CoV-2-RBD-specific antibodies in the immunized group (**Fig. 4p**).

Two contact animals of the OTS-228 group tested positive for the Omicron BA.5 challenge virus in nasal washing samples (**Fig. 4n**), the conchae samples (**Fig. 4o**) and showed reactivity in the serological test (**Fig. 4p**), indicating transmission. The immunized animals exhibited comparable neutralization titers against WT^{D614G}, Omicron BA.2 and BA.5, while the control animals only showed neutralization against Omicron BA.5 (**Fig. 4q**).

Histopathological examination of the lungs showed that the OTS-228 vaccination protected against pneumonia-related atelectasis after challenge with WT, BA.2 or BA.5 (**Supplementary Fig. 2**). However, oligofocal SARS-CoV-2-typical lesions were observed depending on the challenge virus.

Overall, the intranasal single-dose application of OTS-228 was safe and highly effective in providing protection against WT and Omicron BA.2 and BA.5 variants. Importantly, transmission of WT SARS-CoV-2 from OTS-228-immunized animals to contact animals was completely prevented, demonstrating sterile immunity. Additionally, transmission of the Omicron BA.2 and BA.5 VOCs to contact animals was markedly reduced.

Discussion

In this study, we described the first application of the "one-to-stop" strategy to attenuate SARS-CoV-2 to produce safe and effective live attenuated vaccine candidates[2]. By introducing synonymous changes into specific codons, we increased the likelihood of generating nonsense mutations into the viral genome (**Fig. 1a**), leading to reduced viral fitness and efficient attenuation [2]. These modifications had no impact on the amino acid sequence of the viral proteins but made the viruses less fit in primary human airway models (**Fig. 1d,e**).

We demonstrated that the level of attenuation was adjustable by enriching genome regions with additional one-to-stop codons. Through stepwise modifications, we achieved significant attenuation in mice, resulting in 100% survival in a lethal SARS-CoV-2 animal model (**Fig.2a-k**) and marked attenuation in the Syrian hamster model (**Extended Data Fig. 3**). Furthermore, we disarmed the virus by deleting (ORF6-8) and functional knockout specific viral genes (Nsp1:K164A/H165A) known to interfere with antiviral cellular responses (**Fig. 1a**)[19-24].

The resulting live attenuated vaccine candidate, OTS-206, showed optimal attenuation in animal models and provided protection against wild-type SARS-CoV-2, Delta (**Fig. 3**) and the Omicron BA.2 variant (**Fig. 3q-u**). Importantly, OTS-206 immunization led to faster clearance of the Delta variant compared to mRNA vaccines and resolved innate immune responses more rapidly (**Fig. 3b,d**). While sufficient protection against homologues non-Omicron challenge was also shown for other SARS-CoV-2 LAV approaches, like sCPD9[25] or dCOV[26,27], OTS-206 showed that the induced protection sustained for at least five month (**Fig. 3g-m**). The overall protection against the Delta variant was comparable to mRNA vaccines, suggesting that the live attenuated vaccine can also serve as efficient boost of a preexisting immunity.

To further improve the vaccine candidate, we deleted the PCS (PRRAR) resulting in the final candidate, OTS-228 (**Fig. 4a**), which showed a significantly reduced plaque size *in vitro* and limited growth efficiency in hNECs and hBECs (**Fig. 4b,c**). While other SARS-CoV-2 LAV,

exclusively based on either the CPD attenuation concept, with or without having the PCS deletion included[12,25-27], or are based, not on codon sequence modification, but rather on full sequence deletion, e.g. of ORF3, 6, 7 and 8[28] or just the PCS[16]. Therefore, our OTS-228 LAV represents an exceptional candidate, which bundles different attenuation approaches by combining large-scale genome recoding using the OTS concept first time for SARS-CoV-2, targeted deletions (ORF6-8, PCS) and a functional Nsp1 knock-out[3,24]. Besides great *in vivo* attenuation, OTS-228 demonstrated a complete block of transmission in the Syrian hamster model too (**Fig. 4d-j**). In addition to securing genome integrity during vaccine production, we confirmed genome stability by sequencing of *in vitro* passages and *in vivo* samples (**Supplementary Table 5**).

Importantly a single intranasal dose of OTS-228 provided robust protection against severe pathology, prevented virus replication in the lungs, completely blocked transmission of the wild-type virus and significantly reduced transmission of both the Omicron BA.2 and BA.5 variants (**Fig. 4k-r**). These data impressively demonstrate the broad efficacy also against heterologous strains.

In summary, the OTS candidates and particularly OTS-228, are shown to be highly attenuated and safe in pre-clinical animal models. The attenuation is associated with proper replication in the URT, the natural site of SARS-CoV-2 infection, but without transmission or replication in the LRT. Second, the OTS-228 induces protective immune responses against wild-type SARS-CoV-2 and recently emerged Omicron VOCs BA.2 and BA.5. Importantly, as shown for Delta challenge, this level of protection does not decline even 5 months after vaccination. These results highlight the potential of OTS-228 to provide broad and long-lasting immunity against SARS-CoV-2 and its ability to efficiently impede the maintenance of natural transmission chains of an infection with SARS-CoV-2 and emerging variants. Due to its more than

convincing efficacy and innocuousness in preclinical animal models, OTS-228 will now enter the clinical phase.

Methods

Biosafety statement

All experiments with infectious SARS-CoV-2 variants as well as the attenuated OTS constructs were performed in enhanced biosafety level 3 (BSL3) containment laboratories at the Institute of Virology and Immunology (IVI), Mittelhäusern, Switzerland, and Friedrich-Loeffler-Institut (FLI), Greifswald-Insel Riems, Germany. The standard operating procedures of BSL3 facilities were approved by relevant authorities in Switzerland and Germany. All personnel received relevant training before commencing work in BSL3 laboratories.

Ethics statements for animal experimentation

All hamster experiments were evaluated by the responsible ethics committee of the State Office of Agriculture, Food Safety, and Fishery in Mecklenburg–Western Pomerania (LALLF M-V) and gained governmental approval under registration number LVL MV TSD/7221.3-1-041/20. Mouse studies were approved by the Commission for Animal Experimentation of the Cantonal Veterinary Office of Bern and conducted in compliance with the Swiss Animal Welfare legislation and under license BE43/20.

Cell culture

At IVI, VeroE6 (Vero C1008, ATCC) and VeroE6/TMPRSS2 cells (NIBSC Research Reagent Depository, UK) were cultured in Dulbecco's modified Eagle's medium (DMEM) supplemented with 10% (v/v) fetal bovine serum (FBS), 1% (w/v) non-essential amino acids (NEAA), 100 IU/mL penicillin, 100 µg/mL streptomycin µg/ml. BHK-21 cells expressing the N protein of SARS-CoV (BHK-SARS-N)[29] were grown in minimal essential medium (MEM)

supplemented as DMEM above. Cells were maintained at 37 °C with 5% CO_2, under the selection with puromycin (Vero E6/TMPRSS2) and doxycyclin (BHK-SN).

At FLI, VeroE6 (Collection of Cell Lines in Veterinary Medicine CCLV-RIE 0929) were cultured using a mixture of equal volumes of Eagle MEM (Hanks' balanced salts solution) and Eagle MEM (Earle's balanced salts solution) supplemented with 2 mM L-Glutamine, NEAA adjusted to 850 mg/L, $NaHCO_3$, 120 mg/L sodium pyruvate, 10% FBS, pH 7.2.

Generation of infectious cDNA clones using transformation-associated recombination cloning and rescue of recombinant viruses

The in-yeast transformation-associated recombination (TAR) cloning method, as previously described[15], was used to generate recombinant one-to-stop (OTS) viruses of SARS-CoV-2. Briefly, 12 overlapping DNA fragments encoding the entire SARS-CoV-2 genome (referred to as WU-Fragments 1-12), along with a TAR-vector, were recombined in yeast as a yeast artificial chromosome (YAC). WU-Fragments 2, 4, 5, 7, and 8 were recoded according to the OTS strategy to produce OTS-Fragments. The OTS strategy involves recoding all serine and leucine codons to synonymous codons that are just one nucleotide away from encoding a stop codon.

Initially, single OTS fragments were used to create infectious SARS-CoV-2 clones, namely OTS2 (WU-Fragment 2 out of the 12 WU-Fragments was replaced with OTS Fragment 2), OTS4, OTS5, OTS7, OTS8. Subsequently, clones with multiple OTS fragments were created, such as OTS4-5, OTS7-8, and OTS4-5-7-8. **Supplementary Table 3** provides a detailed list of all nucleotide changes recoded in the OTS fragments. The recombinant SARS-CoV-2 OTS-206 infectious clone contains additional modifications, for which we created WU-Fragment 2-Nsp1:K164A,H165A, and WU-Fragment 11:delORF6-8. We introduced four point mutations into WU- Fragment 2 to create amino acid changes K164A and H165A in the Nsp1 gene, and deleted ORF6 to ORF8 from WU-Fragment 11 using PCR. Lastly, to create OTS-228, the final

iteration of our attenuation strategy, WU-Fragment 10 was replaced with WU-Fragment 10:delFCS, where the polybasic cleavage site in the SARS-CoV-2 spike was removed. The primers used for these modifications are listed in **Supplementary Table 2**. The YACs were cleaved by EagI digestion, and *in vitro* transcription was performed using the T7 RiboMAX Large Scale RNA production system (Promega), as previously described[15]. The resulting capped mRNA was electroporated into BHK-21 cells expressing the SARS-CoV N protein. Electroporated BHK-21 cells were then co-cultured with VeroE6/TMPRSS2 cells to produce passage 0 (p.0) of the recombinant viruses. To generate a p.1 virus stock for downstream experiments, the p.0 viruses were used to infect VeroE6/TMPRSS2 cells.

Determination of infectious viral particles, plaque phenotype and foci sizes

A complete list of viruses used in this study can be found in **Supplementary Table 1**. VeroE6 or VeroE6/TMPRSS2 were used to culture viruses, and the identity of all virus stocks was verified by whole-genome NGS sequencing. Infectious viral particle titers were determined by $TCID_{50}$ measurement on VeroE6 or VeroE6/TMPRSS2 cells. Briefly, $2x10^4$ cells/well were seeded in a 96-well plate one day before the titration and were then inoculated with a 10-fold serial dilution of the samples. Three to six technical replicates were performed for each sample. Cells were then incubated at 37°C in a humidified incubator with 5% CO_2. After 72 h, cells were fixed with 4% (v/v) buffered formalin (formafix) and stained with crystal violet. $TCID_{50}$ was calculated according to the Spearman-Kaerber formula. The plaque sizes caused by the respective viruses in 6-well plates 2 days post inoculation were measured in Adobe Illustrator. Statistical significance was determined using ordinary one-way Anova and p-values were adjusted using Tukey's multiple-comparison test; $*P < 0.05$, $**P < 0.01$, $***P < 0.001$, $****P < 0.0001$.

Genetic stability of recombinant OTS viruses

564 To evaluate their genetic stability, OTS4-5 (10-times VeroE6), OTS7-8, (10-times VeroE6)
565 OTS206 (15-times VeroE6/TMPRSS2) were passaged at low MOI (0.01) and sequenced by Ion
566 Torrent Sequencing. Also, conchae samples of OTS4-5 and OTS7-8 contact animals 20 days
567 post initial contact were sequenced. Results are shown in **Supplementary Table 5**.

568 **Ion Torrent Sequencing**

569 Virus stocks and animal samples were sequenced using a generic metagenomics sequencing
570 workflow as described previously[30] with some modifications. For reverse-transcribing RNA
571 into cDNA, SuperScriptIV First-Strand cDNA Synthesis System (Invitrogen, Germany) and
572 the NEBNext Ultra II Non-Directional RNA Second Strand Synthesis Module (New England
573 Biolabs, Germany) were used, and library quantification was done with the QIAseq Library
574 Quant Assay Kit (Qiagen, Germany). Animal samples were treated with a myBaits panel
575 (Daicel Arbor Biosciences) specific for SARS-CoV-2 as described[31]. Libraries were quality-
576 checked, quantified and sequenced using an Ion 530 chip and chemistry for 400 base pair reads
577 on an Ion Torrent S5XL instrument (Thermo Fisher Scientific, Germany). Raw sequencing data
578 were analyzed using the Genome Sequencer Software Suite (version 2.6; Roche, Mannheim,
579 Germany https://roche.com) applying default software settings for quality filtering and
580 mapping. The obtained genome sequences were compared with their reference genomes via
581 alignment using MAFFT version 7.38837, as implemented in Geneious version 10.2.3
582 (Biomatters, Auckland, New Zealand; https://www.geneious.com). The variant analysis
583 integrated in Geneious Prime 10.2.3 were applied (default settings, minimum variant frequency
584 0.02) to detect single nucleotide variants.

585 **Illumina Sequencing**

586 Sequencing reads were trimmed using TrimGalore v.0.6.5 and FastQC v.0.11.9 was used to
587 assess overall read quality. Trimmed reads for each OTS sample were then aligned to their
588 corresponding OTS reference sequence using Bowtie2 v.2.3.4. For virus stocks, consensus

sequences were generated using Samtools v.1.10 with the -d option set to 10,000. For OTS passaged samples, nucleotide variants were called using Lofreq v.2.1.5 with the -C option set to 100 and the -d option set to 10,000. The resulting VCF files were filtered using the lofreq filter command for variants called at a frequency of ≥ 0.1. Data analysis was performed on UBELIX, the high-performance computing (HPC) cluster at the University of Bern (http://www.id.unibe.ch/hpc).

Virus replication kinetics, fluorouracil (5-FU) and molnupiravir treatment

The virus replication kinetics of the OTS viruses in comparison to WT SARS-CoV-2 were determined without any treatment, as well as under fluorouracil (5-FU) (Sigma, F6627) and molnupiravir (Lucerna Chem, HY-135853-10MG) treatment conditions. VeroE6/TMPRSS2 cells were infected with 0.1 MOIs of the WT SARS-CoV-2 or OTS viruses for 1 hour. After an hour, inoculum was removed, cells were washed three times with 1x PBS and new media was added on the cells. Supernatant from wells were collected on 6-, 18-, 24-, 48- and 72-hpi for the infectious virus titer determination and diluted 1:1 with virus transport medium (VTM). For the antiviral treatment condition, VeroE6/TMPRSS2 cells were pretreated for 30 minutes with 5-FU and molnupiravir, and then infected with 0.1 MOI of WT SARS-CoV-2 and OTS4-5-7-8 for 1 hour. Afterwards, inoculum was removed, cells were washed and new medium containing either 5-FU (concentration ranging from 40-280 uM), or molnupiravir (concentration ranging from 0.1 – 10 uM) was added on the cells for 24 hours. After 24 hours, supernatant from cells were collected and used to determine the virus titers. Infectious virus titers were assessed by standard $TCID_{50}$ assays on Vero-E6/TMPRSS2 cells, as explained above.

Well-differentiated primary airway epithelial cells

Primary human bronchial epithelial cells (hBECs) were isolated from lung explants and human nasal epithelial cells (hNECs) were obtained commercially (Epithelix Sàrl). The generation of well-differentiated hBECs and hNECs at the air-liquid interface (ALI) was described previously

614 with minor adjustments[32]. Human BECs/NECs were expanded in collagen-coated (Sigma) cell
615 culture flasks (Costar) in PneumaCult Ex Plus medium, supplemented with 1 µM
616 hydrocortisone, 5 µM Y-27632 (Stem Cell Technologies), 1 µM A-83-01 (Tocris), 3 µM
617 isoproterenol (Abcam), and 100 µg/mL primocin (Invivogen) and maintained at 37°C, 5% CO_2.
618 Expanded hBECs/hNECs were seeded onto 24-well plate inserts with a pore size of 0.4 µm
619 (Greiner Bio-One) at a density of 50'000 cells/insert, submerged into 200 µl of supplemented
620 PneumaCult ExPlus medium on the apical side and 500 µl in the basolateral chamber. To induce
621 the differentiation of the cells, PneumaCult ALI medium supplemented with 4 µg/mL heparin
622 (Stem Cell Technologies), 5 µM hydrocortisone, and 100 µg/mL primocin was added to the
623 basolateral chamber. Basal medium was replaced every 2-3 days and the cells were maintained
624 at 37°C, 5% CO_2 until ciliated cells appeared and mucus was produced. After 3 to 4 weeks post-
625 exposure to ALI, hBECs/hNECs were considered well-differentiated. For figure 1d, well-
626 differentiated hNECs were obtained commercially (Epithelix Sàrl) and consist of a pool of 14
627 human donors each. Basal medium (Epithelix Sàrl) was replaced every 2-3 days and cells were
628 maintained at 33°C, 5% CO_2. To remove mucus from hBECs and hNECs, cells were washed
629 once a week with 250 µl of pre-warmed Hank's balanced salt solution (HBSS, Gibco) for 20
630 min at 37°C.

631 **Virus replication kinetics on human primary airway cells**

632 Human BECs and NECs were infected with $5x10^4$ PFU of the OTS viruses listed or WT SARS-
633 CoV-2 as described previously with some changes[33]. Viruses were diluted in HBSS, applied
634 apically, and incubated for 1 hour at 37°C or 33°C for hBECs or hNECs, respectively. Then,
635 the inoculum was removed, and the cells were washed three times with 100 µl of HBSS. The
636 last wash was collected as the 1 hpi time point and diluted 1:1 with VTM. Afterwards, hBECs
637 and hNECs were incubated in a humidified incubator with 5% CO_2 at 37°C or 33°C,
638 respectively. For quantification of infectious viral particle release 24, 48, 72, and 96 hpi, 100

639 µl HBSS were applied to the apical surface 10 min prior to the respective time point, incubated,
640 and subsequently collected. Apical washes were diluted 1:1 with VTM and stored at -80°C until
641 further analysis. Infectious virus titers in the apical washes were assessed by a standard $TCID_{50}$
642 assay on VeroE6/TMPRSS2 cells.

643 **Mouse studies**

644 A well-characterized SARS-CoV-2 model hACE2-K18Tg mice (Tg(K18-hACE2)2Prlmn)[34,35]
645 were bred at the specific pathogen-free facility of the Institute of Virology and Immunology
646 and housed as previously described[36]. For infection, 7- to 16-week-old female and male mice
647 were anesthetized with isoflurane and inoculated intranasally with 20 µl per nostril (5000
648 PFU/mice). The mice were observed for clinical symptoms, weighed and swabbed at specific
649 time points. The clinical symptoms were scored, and the animals were euthanized before they
650 reached the humane endpoint. On euthanasia day, oropharyngeal swabs, serum and organs
651 samples were harvested as mentioned in our previous studies[35].

652 For the vaccination experiments, K18-hACE2 mice (7–16 weeks old) were immunized twice at
653 a 4-weeks interval either intramuscularly with a single dose of 1 µg of mRNA-Vaccine
654 Spikevax (Moderna) or intranasally with 5'000 PFU of OTS viruses. Four weeks after the boost,
655 the immunized mice and a group of sex- and age-matched naïve animals were challenged
656 intranasally with the challenge virus inoculum (either WT (BetaCoV/Wuhan/IVDC-HB-
657 01/2019, Acc. No. MT108784), WT^{D614G} (BetaCoV/Germany/BavPat1/2020, Acc. No.
658 EPI_ISL_406862) or Delta (hCoV-19/Germany/BW-FR1407/2021, Acc. No.
659 EPI_ISL_2535433)) described in the results section. Euthanasia and organ collection were
660 performed 6 dpc as described above. All mice were monitored daily for body weight loss and
661 clinical signs. Oropharyngeal swabs were collected daily as described before.

662 **Hamster studies**

Specific pathogen free male Syrian golden hamsters (*Mesocricetus auratus*) of 4 – 12 weeks of age were purchased from Janvier labs, Le Genest-Saint-Isle, France. Syrian hamsters received either 70 µl (35 µl into each nostril) of the respective OTS constructs (OTS4-5, OTS7-8, OTS-206 or OTS-228) intranasally or were challenged 3 weeks post immunization with SARS-CoV-2 WT (BetaCoV/Wuhan/IVDC-HB-01/2019, Acc. No. MT108784), , SARS-CoV-2 Omicron BA.2 (SARS-CoV-2/human/NLD/EMC-BA2-1/2022, Acc. No. ON545852, kindly provided by B. Haagmans) or SARS-CoV-2 Omicron BA.5 (hCoV-19/South Africa/CERI-KRISP-K040013/2022, Acc. No. EPI_ISL_12268493.2, kindly provided by Alex Sigal). Details about OTS-viruses and challenge viruses which were used to be found under **Supplementary Table 1**. Body weight was tracked and nasal washing samples, under short term isoflurane anesthesia, were taken (flushing 200 µl PBS into each nostril and collecting the reflux into a 2 mL tube) at time points as specifically indicated for each experiment (**Fig. 2l, r; Fig. 4d, k; Extended Data Fig. 3a; Extended Data Fig. 8, Extended Data Fig. 9**). To obtain organ samples (nasal conchae, trachea, lung caudal, medial and cranial) animals were euthanized by an isoflurane overdose and subsequent decapitation. Serum samples were obtained during euthanasia by collecting the blood into serum separating tubes (BD Vacutainer™).

Processing of animal specimens, viral RNA and infectious particle quantification

Organ samples of about 0,1 cm^3 size from hamsters were homogenized in a 1 mL mixture composed of equal volumes of Hank's balanced salts MEM and Earle's balanced salts MEM containing 2 mM L-glutamine, 850 mg l−1 $NaHCO_3$, 120 mg l−1 sodium pyruvate, and 1% penicillin–streptomycin) at 300 Hz for 2 min using a Tissuelyser II (Qiagen) and were then centrifuged to clarify the supernatant.

Nucleic acid was extracted from 100 µl of the nasal washes of hamsters after a short centrifugation step or 100 µl of organ sample supernatant using the NucleoMag Vet kit (Macherey Nagel). Nasal washings, oropharyngeal swabs and organ samples from hamsters

were tested by virus-specific RT-qPCR. The RT-qPCR reaction was prepared using the qScript XLT One-Step RT-qPCR ToughMix (QuantaBio, Beverly, MA, USA) in a volume of 12.5 µl including 1 µl of the respective FAM mix and 2.5 µl of extracted RNA. The reaction was performed for 10 min at 50°C for reverse transcription, 1 min at 95°C for activation, and 42 cycles of 10 sec at 95°C for denaturation, 10 sec at 60°C for annealing and 20 sec at 68°C for elongation. Fluorescence was measured during the annealing phase. RT-qPCRs were performed on a BioRad real-time CFX96 detection system (Bio-Rad, Hercules, USA). The primers are listed in **Supplementary Table 2**.

Organ samples from mice were either homogenized in 0.5 mL of RA1 lysis buffer supplemented with 1% β-mercaptoethanol and later used for RNA isolation, or in 1 ml DMEM containing gentleMACS M-tubes (Miltenyi Biotec) for the detection of infectious particles as described before[36]. RNA was isolated using the NucleoMag Vet kit (Macherey Nagel). The RT-qPCR reaction was prepared using TaqPath™ 1 Step Multiplex Master Mix kit (Thermofisher) with primers and probes targeting SARS-CoV-2 E gene, and was performed for 10 min at 45°C for reverse transcription, 10 min at 95°C for activation, and 45 cycles of 15 sec at 95°C for denaturation, 30 sec at 58°C for annealing and 30 sec at 72°C for elongation. Fluorescence was measured during the annealing phase. RT-qPCRs were performed on a BioRad real-time CFX96 detection system (Bio-Rad, Hercules, USA). The primers are listed in **Supplementary Table 2**. Infectious virus titers were determined by $TCID_{50}$ measurement on VeroE6 cells and were calculated according to the Spearman-Kaerber formula.

Histopathological and immunohistochemical analysis

Mice

The left lung and the left hemisphere of the brain from mice were collected into 4% formalin. After fixation, both tissues were embedded in paraffin, cut at 4 µm and stained with hematoxylin and eosin (H&E) for histological evaluation. Scoring of the lung tissue pathology

was done according to a previously published scoring scheme [36]. Immunohistochemical (IHC) analysis of the lung and the brain was performed by using a rabbit polyclonal anti-SARS-CoV nucleocapsid antibody (Rockland, 200-401-A50) in a BOND RXm immunostainer (Leica Byosystems, Germany). For that purpose, paraffin blocks were cut at 3 µm, incubated with citrate buffer for 30 min at 100°C for antigen retrieval, and incubated with a 1:3000 dilution of the first antibody for 30 min at room temperature. BondTM Polymer Refine Detection visualisation kit (Leica Byosystems, Germany) was afterwards used for signal detection using DAB as chromogen and counterstaining with hematoxylin.

Hamster

The left lung lobe was carefully removed, immersion-fixed in 10% neutral-buffered formalin, paraffin-embedded, and 2–3-µm sections were stained with hematoxylin and eosin (HE). Consecutive sections were processed for immunohistochemistry (IHC) used according to standardized procedures of avidin-biotin-peroxidase complex (ABC)-method. Briefly, endogenous peroxidase was quenched on dewaxed lung slides with 3% hydrogen peroxide in distilled water for 10 minutes at room temperature (RT). Antigen heat retrieval was performed in 10 mM citrate buffer (pH 6) for 20 minutes in a pressure cooker. Nonspecific antibody binding was blocked for 30 minutes at RT with goat normal serum, diluted in PBS (1:2). A primary anti-SARS-CoV nucleocapsid protein antibody was applied overnight at 4°C (Rockland, 200-401-A50, 1:3000), the secondary biotinylated goat anti-mouse antibody was applied for 30 minutes at room temperature (Vector Laboratories, Burlingame, CA, USA, 1:200). Color was developed by incubation with ABC solution (Vectastain Elite ABC Kit; Vector Laboratories), followed by exposure to 3-amino-9-ethylcarbazole substrate (AEC, Dako, Carpinteria, CA, USA). The sections were counterstained with Mayer's haematoxylin and cover slipped. As negative control, consecutive sections were labelled with an irrelevant antibody (M protein of Influenza A virus, ATCC clone HB-64). An archived control slide from

738 a SARS-CoV2 infected Syrian hamster was included in each run. All slides were scanned using
739 a Hamamatsu S60 scanner and evaluated using the NDPview.2 plus software (Version 2.8.24,
740 Hamamatsu Photonics, K.K. Japan) by a trained (TB) and board-certified pathologist (AB),
741 blind to treatment. The lung tissue was evaluated using a 500 × 500 µm grid, and the extent of
742 pneumonia-associated consolidation was recorded as percentage of affected lung fields.
743 Further, the lung was examined for the presence of SARS-CoV-2-characteristic lesions
744 described for hamsters, i.e. intra-alveolar, interstitial, peribronchial and perivascular
745 inflammatory infiltrates, alveolar edema, necrosis of the bronchial epithelium, diffuse alveolar
746 damage, vasculitis, activation of endothelium with immune cell rolling, as well as bronchial
747 epithelial and pneumocyte type 2 hyperplasia. Following IHC the distribution of virus antigen
748 was graded on an ordinal scale with scores 0 = no antigen, 1 = focal, affected cells/tissue <5%
749 or up to 3 foci per tissue; 2 = multifocal, 6%–40% affected; 3 = coalescing, 41%–80% affected;
750 4 = diffuse, >80% affected. The target cell was identified based on morphology.

751 **Serological tests**

752 To evaluate the virus neutralizing potential of hamster serum samples, a live virus neutralization
753 test was done following an established standard protocol as described before[37]. Briefly, sera
754 were prediluted 1/16 in MEM and further diluted in log2 steps until a final tested dilution of
755 1/4096. Each dilution was evaluated for its potential to prevent 100 $TCID_{50}$ SARS-CoV-2/well
756 of the respective VOC from inducing cytopathic effect in Vero E6 cells, giving the virus
757 neutralization titer (VNT_{100}). Following SARS-CoV-2 variants were used to test against:
758 SARS-CoV-2 WT^{D614G} (BetaCoV/Germany/BavPat1/2020, Acc. No. EPI_ISL_406862, kindly
759 provided by Roman Wölfel), SARS-CoV-2 Omicron BA.2 (SARS-CoV-2/human/NLD/EMC-
760 BA2-1/2022, Acc. No. ON545852, kindly provided by B. Haagmans) or SARS-CoV-2
761 Omicron BA.5 (hCoV-19/South Africa/CERI-KRISP-K040013/2022, Acc. No.
762 EPI_ISL_12268493.2, kindly provided by Alex Sigal).

763 Additionally, serum samples were tested by multispecies ELISA for sero-reactivity against the
764 WT SARS-CoV-2 RBD domain[38].

765 Similarly, for mouse samples, serum was diluted initially at 1:20 with DMEM, and
766 subsequently was further diluted to reach the final dilution of 1:2560. Diluted sera were first
767 incubated with the virus in 1:1 volume ratio, and after 1h incubation, the serum-virus mixture
768 was applied on Vero E6 cells in 96-well plates for 2-3 days incubation period. The serum
769 dilution in which the cells were still intact was recorded as neutralization titer of the serum for
770 the given virus.

771 **Spatial transcriptomics and gene expression analysis**

772 5µm thick formalin-fixed paraffin-embedded (FFPE) lung tissue sections were placed on
773 Visium Spatial Gene Expression slides (10X Genomics) containing four capture areas each and
774 processed according to the manufacturer's recommendations. In addition to the mouse
775 transcriptome probes, we designed probes for the SARS-CoV-2 virus targeting ORF1ab,
776 ORF3a, ORF10, and the genes encoding the structural proteins spike (S), envelope (E),
777 membrane (M), and nucleocapsid (N). The custom SARS-CoV-2 probes are listed in
778 **Supplementary Table 4** and the final concentration for each primer in the probe hybridization
779 mix was 1.2 nM. The cDNA libraries were loaded onto the NovaSeq 6000 (Illumina) and
780 sequenced with a minimum of 50,000 reads per covered spot. Reads contained in Illumina
781 FASTQ files were aligned to a custom multi-species reference transcriptome generated with
782 Space Ranger using the GRCm38 (version mm10-2020-A_build, 10X Genomics) mouse and
783 NC_045512.2 SARS-CoV-2 references. Downstream data analysis of the mouse samples was
784 performed using SCANPY[39]. To compare host and viral gene expression levels across
785 conditions, the counts were first normalized and then log transformed. To examine spatial
786 correlations between total viral mRNA counts and host genes, pairwise Pearson's correlation

coefficients were calculated and compared across conditions. Cellular pathway activity scores for 13 different cellular pathways were calculated using PROGENy[40].

Statistical analysis, readability and figures

Statistical analysis was performed using GraphPad Prism 9 (Version 9.5.1). Unless noted otherwise, the results are expressed as mean ± s.d. Specific tests are indicated in the main text or the figure legends. LLM (openai.com) was used to improve readability and shorten the original text. Schematic overviews for animal experiments were created with BioRender.com.

References

1 Markov, P. V. *et al.* The evolution of SARS-CoV-2. *Nat Rev Microbiol* **21**, 361-379, doi:10.1038/s41579-023-00878-2 (2023).

2 Moratorio, G. *et al.* Attenuation of RNA viruses by redirecting their evolution in sequence space. *Nat Microbiol* **2**, 17088, doi:10.1038/nmicrobiol.2017.88 (2017).

3 Mendez, A. S. *et al.* The N-terminal domain of SARS-CoV-2 nsp1 plays key roles in suppression of cellular gene expression and preservation of viral gene expression. *Cell Rep* **37**, 109841, doi:10.1016/j.celrep.2021.109841 (2021).

4 Cao, Z. *et al.* Ubiquitination of SARS-CoV-2 ORF7a promotes antagonism of interferon response. *Cell Mol Immunol* **18**, 746-748, doi:10.1038/s41423-020-00603-6 (2021).

5 Li, J. Y. *et al.* The ORF6, ORF8 and nucleocapsid proteins of SARS-CoV-2 inhibit type I interferon signaling pathway. *Virus Res* **286**, 198074, doi:10.1016/j.virusres.2020.198074 (2020).

6 Xia, H. *et al.* Evasion of Type I Interferon by SARS-CoV-2. *Cell Rep* **33**, 108234, doi:10.1016/j.celrep.2020.108234 (2020).

7 Zhang, Y. *et al.* The ORF8 protein of SARS-CoV-2 mediates immune evasion through down-regulating MHC-Iota. *Proc Natl Acad Sci U S A* **118**, doi:10.1073/pnas.2024202118 (2021).

8 Miorin, L. *et al.* SARS-CoV-2 Orf6 hijacks Nup98 to block STAT nuclear import and antagonize interferon signaling. *Proc Natl Acad Sci U S A* **117**, 28344-28354, doi:10.1073/pnas.2016650117 (2020).

9 Kimura, I. *et al.* Sarbecovirus ORF6 proteins hamper induction of interferon signaling. *Cell Rep* **34**, 108916, doi:10.1016/j.celrep.2021.108916 (2021).

10 Kato, K. *et al.* Overexpression of SARS-CoV-2 protein ORF6 dislocates RAE1 and NUP98 from the nuclear pore complex. *Biochem Biophys Res Commun* **536**, 59-66, doi:10.1016/j.bbrc.2020.11.115 (2021).

11 Addetia, A. *et al.* SARS-CoV-2 ORF6 Disrupts Bidirectional Nucleocytoplasmic Transport through Interactions with Rae1 and Nup98. *mBio* **12**, doi:10.1128/mBio.00065-21 (2021).

12 Adler, J. M. *et al.* A non-transmissible live attenuated SARS-CoV-2 vaccine. *Mol Ther*, doi:10.1016/j.ymthe.2023.05.004 (2023).

13 Peacock, T. P. *et al.* The furin cleavage site in the SARS-CoV-2 spike protein is required for transmission in ferrets. *Nat Microbiol* **6**, 899-909, doi:10.1038/s41564-021-00908-w (2021).

14 Hoffmann, M., Kleine-Weber, H. & Pohlmann, S. A Multibasic Cleavage Site in the Spike Protein of SARS-CoV-2 Is Essential for Infection of Human Lung Cells. *Mol Cell* **78**, 779-784 e775, doi:10.1016/j.molcel.2020.04.022 (2020).

15 Thi Nhu Thao, T. *et al.* Rapid reconstruction of SARS-CoV-2 using a synthetic genomics platform. *Nature* **582**, 561-565, doi:10.1038/s41586-020-2294-9

10.1038/s41586-020-2294-9 [pii] (2020).
16 Johnson, B. A. *et al.* Loss of furin cleavage site attenuates SARS-CoV-2 pathogenesis. *Nature* **591**, 293-299, doi:10.1038/s41586-021-03237-4 (2021).
17 Callahan, V. *et al.* The Pro-Inflammatory Chemokines CXCL9, CXCL10 and CXCL11 Are Upregulated Following SARS-CoV-2 Infection in an AKT-Dependent Manner. *Viruses* **13**, doi:10.3390/v13061062 (2021).
18 Ferreira-Gomes, M. *et al.* SARS-CoV-2 in severe COVID-19 induces a TGF-beta-dominated chronic immune response that does not target itself. *Nat Commun* **12**, 1961, doi:10.1038/s41467-021-22210-3 (2021).
19 Fisher, D. G., Gnazzo, V., Holthausen, D. J. & Lopez, C. B. Non-standard viral genome-derived RNA activates TLR3 and type I IFN signaling to induce cDC1-dependent CD8+ T-cell responses during vaccination in mice. *Vaccine* **40**, 7270-7279, doi:10.1016/j.vaccine.2022.10.052 (2022).
20 Kovac, A. *et al.* Misfolded truncated protein tau induces innate immune response via MAPK pathway. *J Immunol* **187**, 2732-2739, doi:10.4049/jimmunol.1100216 (2011).
21 Dabaghian, M., Latifi, A. M., Tebianian, M., Dabaghian, F. & Ebrahimi, S. M. A truncated C-terminal fragment of Mycobacterium tuberculosis HSP70 enhances cell-mediated immune response and longevity of the total IgG to influenza A virus M2e protein in mice. *Antiviral Res* **120**, 23-31, doi:10.1016/j.antiviral.2015.05.002 (2015).
22 Yount, J. S., Kraus, T. A., Horvath, C. M., Moran, T. M. & Lopez, C. B. A novel role for viral-defective interfering particles in enhancing dendritic cell maturation. *J Immunol* **177**, 4503-4513, doi:10.4049/jimmunol.177.7.4503 (2006).
23 Tapia, K. *et al.* Defective viral genomes arising in vivo provide critical danger signals for the triggering of lung antiviral immunity. *PLoS Pathog* **9**, e1003703, doi:10.1371/journal.ppat.1003703 (2013).
24 Thoms, M. *et al.* Structural basis for translational shutdown and immune evasion by the Nsp1 protein of SARS-CoV-2. *Science* **369**, 1249-1255, doi:10.1126/science.abc8665 (2020).
25 Nouailles, G. *et al.* Live-attenuated vaccine sCPD9 elicits superior mucosal and systemic immunity to SARS-CoV-2 variants in hamsters. *Nat Microbiol* **8**, 860-874, doi:10.1038/s41564-023-01352-8 (2023).
26 Mehla, R. *et al.* A Live Attenuated COVID-19 Candidate Vaccine for Children: Protection against SARS-CoV-2 Challenge in Hamsters. *Vaccines (Basel)* **11**, doi:10.3390/vaccines11020255 (2023).
27 Wang, Y. *et al.* Scalable live-attenuated SARS-CoV-2 vaccine candidate demonstrates preclinical safety and efficacy. *Proc Natl Acad Sci U S A* **118**, doi:10.1073/pnas.2102775118 (2021).
28 Liu, Y. *et al.* A live-attenuated SARS-CoV-2 vaccine candidate with accessory protein deletions. *Nat Commun* **13**, 4337, doi:10.1038/s41467-022-31930-z (2022).
29 van den Worm, S. H. *et al.* Reverse genetics of SARS-related coronavirus using vaccinia virus-based recombination. *PLoS One* **7**, e32857, doi:10.1371/journal.pone.0032857

PONE-D-11-21011 [pii] (2012).
30 Wylezich, C., Papa, A., Beer, M. & HÃ¶per, D. A Versatile Sample Processing Workflow for Metagenomic Pathogen Detection. *Scientific Reports* **8**, 13108, doi:10.1038/s41598-018-31496-1 (2018).
31 Wylezich, C. *et al.* Next-generation diagnostics: virus capture facilitates a sensitive viral diagnosis for epizootic and zoonotic pathogens including SARS-CoV-2. *Microbiome* **9**, 51, doi:10.1186/s40168-020-00973-z (2021).
32 Fahmi, A. *et al.* SARS-CoV-2 can infect and propagate in human placenta explants. *Cell Rep Med* **2**, 100456, doi:10.1016/j.xcrm.2021.100456

S2666-3791(21)00324-4 [pii] (2021).
33 Barut, G. T. *et al.* The spike gene is a major determinant for the SARS-CoV-2 Omicron-BA.1 phenotype. *Nat Commun* **13**, 5929, doi:10.1038/s41467-022-33632-y (2022).

34 McCray, P. B., Jr. *et al.* Lethal infection of K18-hACE2 mice infected with severe acute respiratory syndrome coronavirus. *J Virol* **81**, 813-821, doi:JVI.02012-06 [pii]

10.1128/JVI.02012-06 (2007).

35 Zhou, B. *et al.* SARS-CoV-2 spike D614G change enhances replication and transmission. *Nature* **592**, 122-127, doi:10.1038/s41586-021-03361-1

10.1038/s41586-021-03361-1 [pii] (2021).

36 Ulrich, L. *et al.* Enhanced fitness of SARS-CoV-2 variant of concern Alpha but not Beta. *Nature* **602**, 307-313, doi:10.1038/s41586-021-04342-0

10.1038/s41586-021-04342-0 [pii] (2022).

37 Schlottau, K. *et al.* SARS-CoV-2 in fruit bats, ferrets, pigs, and chickens: an experimental transmission study. *Lancet Microbe* **1**, e218-e225, doi:10.1016/S2666-5247(20)30089-6 (2020).

38 Wernike, K. *et al.* Multi-species ELISA for the detection of antibodies against SARS-CoV-2 in animals. *Transbound Emerg Dis* **68**, 1779-1785, doi:10.1111/tbed.13926 (2021).

39 Wolf, F. A., Angerer, P. & Theis, F. J. SCANPY: large-scale single-cell gene expression data analysis. *Genome Biol* **19**, 15, doi:10.1186/s13059-017-1382-0 (2018).

40 Schubert, M. *et al.* Perturbation-response genes reveal signaling footprints in cancer gene expression. *Nat Commun* **9**, 20, doi:10.1038/s41467-017-02391-6 (2018).

Acknowledgment

We thank the NIH Tetramer Core Facility (contract number 75N93020D00005) for providing tetramers (H-2K(b) SARS-CoV-2 S 539-546 VNFNFNGL and H-2D(b) Influenza A NP 366-374 ASNENMETM). We thank Dr. Hiu Ying Stoller and Ursula Romanelli for providing us with the mRNA vaccine. This project was supported in part by the Novartis Foundation for Medical-Biological Research (grant 22B099 to Dr. Etori Aguiar Moreira). We thank Swiss National Science Foundation (SNSF) grant no. 31CA30_196062 (CB) for funding. We thank the Next Generation Sequencing Platform of the University of Bern for performing the high-throughput sequencing experiments, and the COMPATH platform of the Institute of Pathology and Institute of Animal Pathology, University of Bern for performing the pathological analyses. VeroE6/TMPRSS2 cells were provided by the NIBSC Research Reagent Repository, UK, thanks to Dr Makoto Takeda. We thank Mareen Grawe for excellent technical assistance with the hamster experiments, Robin Brandt for excellent technical assistance with the pathological

912 analyses, and Patrick Zitzow and Lukas Wessler for excellent technical assistance with the next-
913 generation sequencing.

914 **Competing interests**

915 Related to this work, the University of Bern has filed a patent application for the use of OTS-
916 206 and OTS-228 as vaccine. In this application, J.S., G.T.B., B.S.T., N.J.H., A.K., L.U., F.L.,
917 J.J., N.E., D.H., M.B., and V.T. are named as inventors. The University of Bern and the
918 Friedrich-Loeffler Institute are collaborating with RocketVax AG for the development of OTS
919 vaccines and receive funding for research. V.T. is consulting for RocketVax AG. P.V. and V.C.
920 are employees of RocketVax AG.

921 **Author contributions**

922 Conceptualization: M.B., V.T., N.E., D.H., P.V., V.C.; Methodology: M.B., V.T., N.E., D.H.;
923 Validation: M.B., V.T., N.E., D.H.; Formal analysis: J.S., G.T.B., B.S.T., J.N.K., E.A.M.,
924 C.W.; Investigation: J.S., G.T.B., B.S.T., N.J.H., I.B.V., A.K., L.U., J.N.K., M.Br., C.W., A.T.,
925 E.A.M., P.D.T., L.G.-R., K.S., T.B., A.B., B.O.E., L.A., L.T., C.D., S.S., S.O., Ki.S., F.L., J.J.,
926 M.P.A., C.B., D.H., N.E., H.S.; Data curation: G.T.B., J.S., C.W., J.N.K., E.A.M., A.A.;
927 Writing—original draft preparation: G.T.B., J.S., B.S.T., J.N.K., A.K., A.B., M.B., V.T., D.H.;
928 Writing - Review & Editing: G.T.B., J.S., B.S.T., M.B., V.T., J.J., F.L., C.B., A.K., N.J.H,
929 J.N.K., M.Br., C.W., A.T., E.A.M., P.D.T, L.G.R, A.B., L.T., C.D., D.H., N.E., H.S.;
930 Visualization: G.T.B., J.S., B.S.T., E.A.M.; Supervision: V.T., M.B., D.H., N.E., Project
931 administration: V.T., M.B.; Funding acquisition: V.T., M.B., C.B. All authors have critically
932 reviewed and agreed to the published version of the manuscript.

933 **Data availability**

934 All data are available in the main text or the supplementary materials. Source data are provided
935 with this paper. The project information is accessible with the BioProject ID PRJNA.

Supplementary Files

This is a list of supplementary files associated with this preprint. Click to download.

- SupplementaryData.pdf
- ExtendedData.pdf